

Research Paper

Sphingomyelin Liposomes Containing Porphyrin–phospholipid for Irinotecan Chemophototherapy

Kevin A Carter¹, Dandan Luo¹, Aida Razi², Jumin Geng¹, Shuai Shao¹, Joaquin Ortega², Jonathan F Lovell¹✉

1. Department of Biomedical Engineering, University at Buffalo, State University of New York, Buffalo, NY, 14260.

2. Department of Biochemistry and Biomedical Sciences and M. G. DeGroot Institute for Infectious Diseases Research, McMaster University, Hamilton, ON L8S4L8, Canada.

✉ Corresponding author: jflovell@buffalo.edu

© Ivyspring International Publisher. Reproduction is permitted for personal, noncommercial use, provided that the article is in whole, unmodified, and properly cited. See <http://ivyspring.com/terms> for terms and conditions.

Received: 2016.03.30; Accepted: 2016.06.24; Published: 2016.10.01

Abstract

Porphyrin–phospholipid (PoP) liposomes can entrap anti-cancer agents and release them in response to near infrared (NIR) light. Doxorubicin, when remotely loaded via an ammonium sulfate gradient at a high drug-to-lipid ratio, formed elongated crystals that altered liposome morphology and could not be loaded into liposomes with higher PoP content. On the other hand, irinotecan could also be remotely loaded but did not form large crystals and did not induce liposome elongation. The loading, stability, and NIR light-triggered release of irinotecan in PoP liposomes was altered by the types of lipids used and the presence of PEGylation. Sphingomyelin, which has been explored previously for liposomal irinotecan, was found to produce liposomes with relatively improved serum stability and rapid NIR light-triggered drug release. PoP liposomes composed from sphingomyelin, cholesterol and 2 molar percent PoP rapidly released irinotecan in vivo in response to NIR irradiation as monitored by intravital microscopy and also induced effective tumor eradication in mice bearing MIA Paca-2 subcutaneous tumor xenografts.

Key words: liposomes, chemophototherapy, irinotecan

Introduction

Liposomes have been used successfully as pharmaceutical carriers for anti-cancer agents [1,2]. Encapsulating chemotherapy agents in liposomes can reduce non-specific toxicity, and enhance the therapeutic effects of the drug [3,4]. Most of the nanoparticles currently being used for the treatment of solid tumors rely on the enhanced permeability and retention (EPR) effect for drug accumulation in the tumor [4,5]. This effect allows particles of a specific size range to passively accumulate due to the leaky nature of blood vessels in tumors [6–8]. Doxil[®], a long circulating PEGylated liposomal form of doxorubicin takes advantage of this effect. PEGylated liposomes circulate for extended durations, which in turn allows for more passive accumulation of the drug in the tumor [5–9]. While the EPR effect can be exploited for the treatment of certain tumors clinically, the success of drug delivery strategies which rely on the EPR

effect has been limited. This is due to other factors such as high interstitial fluid pressure, poor vascularization in the tumor, tumor heterogeneity, and poor drug bioavailability [10–13]. Several strategies have been proposed to overcome these limitations including active targeting, and site specific release of nanoparticle-encapsulated drugs, with varying degrees of success [14–18]. Site-specific triggered drug release is of interest as it provides the ability to increase the bioavailability of nanoparticle encapsulated drugs at the tumor site improving the efficacy of the treatment. The use of light to induce enhanced drug deposition is an emerging area of research [19–26]. Such combination of chemotherapy and phototherapy; chemophototherapy, is a developing treatment modality for solid tumors. [27] Porphyrins and other tetrapyrroles are promising candidates for phototherapy applications.[28–30] We

have recently found that porphyrin-phospholipids are well-suited to be used for theranostic applications, including chemophototherapy [31–40].

It was shown that PEGylated liposomes containing porphyrin-phospholipid (PoP) enable near infrared (NIR) light-triggered drug release and have a significant therapeutic effect on tumor xenografts using different types of PoP including 2-[1-hexyloxyethyl]-2-devinyl pyropheophorbide-*a* (HPPH-lipid) [31,32] and pyropheophorbide-*a* (pyro-lipid) [33]. At a high PoP molar percentage in the liposome bilayer, HPPH-lipid was originally shown to be more effective at entrapping both dyes and the anti-cancer drug doxorubicin (Dox) than pyro-lipid [31,34]. However, follow-up studies have shown that pyro-lipid, when used with specific liposomal formulations at lower PoP molar percentage in the bilayer, gives rise to greater serum stability. While liposomes made with pyro-lipid were more stable than HPPH-lipid, the amount of pyro-lipid which could be used while retaining Dox loading capacity was limited by the cholesterol content [33]. With lower cholesterol content (i.e. 35 mol. %) Dox could not be loaded into liposomes containing more than 2 mol. % pyro-lipid whereas liposomes made with 45 mol. % cholesterol could be loaded with Dox with up to 8 mol. % pyro-lipid. The exact reason for this trend was not ascertained, however the physical stress imparted on the bilayer due to large Dox exerting physical pressure may be responsible. With high amounts of Dox loading into liposomes, the morphology is known to convert from spherical to ellipsoid [41–43]. This stretching may cause the bilayer of liposomes containing higher amounts of pyro-lipid to become destabilized.

Irinotecan hydrochloride (IRT, CPT-11) is a water soluble topoisomerase I inhibitor which gets converted to its active form SN-38 *in vivo* [44]. Liposomal irinotecan has been shown to be effective. [45,46] It is used clinically in both its free and liposomal form [47,48]. Unlike Dox, IRT does not form large elongated crystals when actively loaded [49,50]. Here we show that, IRT can be loaded in sphingomyelin liposomes and be used for light-triggered drug release and anti-tumor effective chemophototherapy.

2. Methods

2.1 Liposome preparation

Unless otherwise noted, lipids were purchased from Avanti Polar Lipids, and other materials were obtained from Sigma. 1,2-distearoyl-sn-glycero-3-phosphocholine (DSPC, Avanti #850365P), cholesterol (Avanti #700000P), 1,2-distearoyl-sn-glycero-3-

phosphoethanolamine-N-[methoxy(polyethylene glycol)-2000] (DSPE-PEG-2K, Avanti #880120P), and Sphingomyelin (SPM, # Coatsome NM-10, NOF America) were used. Pyro-lipid was synthesized as previously reported [34]. Liposomes were made by dissolving the lipids (100 mg) of the indicated compositions in 1 mL of ethanol at 60°C and 4 mL of 250 mM ammonium sulfate (60°C) was added to the ethanol solution. The liposomes were then extruded 10 times in a high pressure nitrogen extruder (Northern Lipids) using stacked (80, 100 and 200 nm) polycarbonate membranes at 60°C. Free ammonium sulfate and ethanol were removed by dialysis with a 10% sucrose, 10 mM histidine (pH 6.5) solution overnight. IRT (LC Laboratories # I-4122) or Dox (LC Laboratories # D-4000) were loaded into the liposomes by mixing the liposomes and drug in the indicated ratios and incubating the solution for 60 minutes at 60°C. For serum stability studies, liposomes were made with either SPM:pyro-lipid:chol (53:2:45), or with SPM:DSPE-PEG2000:pyro-lipid:chol (48:5:2:45), or with DSPC:DSPE-PEG2000:pyro-lipid:chol (48:5:2:45).

2.2 Liposome characterization

Liposome size and zeta potential were measured by dynamic light scattering in a NanoBrook 90 plus PALS instrument. Sizes were measured in PBS and zeta potential in a 1 mM NaCl solution. Loading efficiency was characterized by running the samples through a Sephadex G-75 column and collecting 24 × 1 mL fractions. The loading efficiency was determined by the amount of drug fluorescence in the liposome-containing fractions. IRT fluorescence was measured an excitation of 370 nm and emission of 435 nm using a TECAN Safire fluorescent microplate reader. Stability was tested in 50% bovine serum at 37°C. IRT fluorescence was measured at the indicated time points and the % release was calculated using the formula $\text{Release} = (F_{\text{final}} - F_{\text{initial}}) / (F_{\text{TX-100}} - F_{\text{initial}}) \times 100\%$, where $F_{\text{TX-100}}$ is the fluorescence value when the liposomes are lysed with 0.25% Triton X-100.

2.3 Light release experiments

Release tests were conducted at 37°C in 50% bovine serum unless otherwise noted. Liposome samples were diluted 1000 times and irradiated using a 665 nm diode laser (RPMC laser, LDX-3115-665) at a fluence rate of ~310 mW/cm². IRT release was measured in real time in a fluorometer (PTI) and the percent release was calculated by the formula $\text{Release} = (F_{\text{final}} - F_{\text{initial}}) / (F_{\text{TX-100}} - F_{\text{initial}}) \times 100\%$

2.4 Cyro-TEM

Holey carbon grids (c-flat CF-2/2-2C-T) were treated with chloroform for ~ 10 hours and then glow

discharged at 5 mA for 15 seconds immediately before the application of the sample. IRT- and Dox PoP-liposomes at a concentration of ~20 mg/mL (lipid) were diluted 10x with water. Approximately 4 μ L of the diluted preparation were deposited on the electron microscopy grid. Vitrification of samples was performed in a Vitrobot (FEI) by blotting the grids once for 15 seconds and with 0 offset before they were plunged into liquid ethane. Temperature and relative humidity during the vitrification process were maintained at 25 °C and 100%, respectively. The grid was loaded into the FEI Tecnai F20 electron microscope operated at 200kV using a Gatan 626 single tilt cryo-holder. Images were collected in a Gatan K2 Summit direct detector device camera at a nominal magnification 25,000X, which produced images with a calibrated pixel size of 1.45Å. The detector was used in counting movie mode with five electrons per pixel per second with 15 second exposures and 0.5 seconds per frame. This method produced movies containing 30 frames with an exposure rate of one electron per square angstrom per frame. Movies were collected using a defocus range of -1 to -2.5 μ m. Frames were aligned using the program `alignframesleastsquares_list.exe` and averaged into a single micrograph with the `shiftframes_list.exe` program available from the website of Dr. John Rubinstein. These programs perform whole frame alignment of the movies using previously published motion correction algorithms [51]. A de-noising filter using Photoshop was applied to the entire image to obtain the figures shown.

2.5 Animal studies

Procedures performed were approved by the University at Buffalo Institutional Animal Care and Use Committee. 5×10^6 Mia Paca-2 cells (obtained from ATCC) were injected in the right flank female nude mice (5 weeks, Jackson Labs, #007850). When tumor volumes reached 5-7 mm in diameter, mice bearing Mia Paca-2 tumors were grouped as follows: 1) Saline, Free IRT, PoP(IRT)-laser, PoP(empty)+laser, PoP(IRT)+laser (n=5-7 mice per group). Mice were injected with 15 mg/kg free IRT, PoP(IRT) or empty PoP-liposomes of an equivalent PoP dose. 10-15 minutes following injection, mice in the +laser groups were treated with a 665 nm laser for 16 min. 40 sec. at a fluence rate of 300 mW/cm². Tumor volumes were measured 2-3 times per week and volumes were calculated using the equation $\text{Volume} = \pi \times L \times W \times H / 6$ where L, W and H represent the length, width and height respectively. The mice were sacrificed when the tumor volume reached 10 times the initial size.

For intravital imaging, female nude mice were injected with IRT-loaded PoP liposomes (10 mg/kg)

or co-injected with standard liposomes and empty PoP liposomes for an equivalent IRT or pyro-lipid dose. The mice were anesthetized using isoflurane and one ear of the mouse was treated with a 665 nm laser for 16.4 minutes at a fluence rate of 300 mW/cm². Following the laser treatment both the treated and untreated ears were imaged using a fluorescent microscope (EVOS FL Auto). IRT was imaged using a DAPI filter cube (357 nm excitation; 477 nm emission) and pyro was imaged with a custom filter cube (400 nm excitation; 679 nm emission).

2.7 Statistical analysis

Kaplan-Meier survival curves were analyzed using Graphpad prism (Version 5.01) software. Groups were compared by Log-rank (Mantel-Cox) test. Differences were considered significant at $p < 0.05$. Median survival was defined as the time at which the survival curve crossed the 50% survival point.

3. Results and Discussion

3.1 Drug loading and release

We recently reported a long-circulating stealth liposomal Dox formulation that contained a small amount of pyro-lipid and exhibited similar pharmacokinetics to the pyro-lipid free liposomes, while being effective for chemophototherapy [33]. However, there was a maximum amount of pyro-lipid which could be added to the liposomes before Dox loading became impossible. To examine if this phenomenon occurred with irinotecan (IRT), liposomes were prepared with DSPC:DSPE-PEG2000:Cholesterol (molar ratio 60:5:35) and pyro-lipid was titrated in, replacing DSPC. As expected, Dox could not be loaded into liposomes containing more than 2 mol. % pyro-lipid; IRT however did not show such limitations and could be loaded into liposomes containing as much as 15 mol. % pyro-lipid. (**Fig 1A**). The NIR light-triggered release of IRT was tested using 2 mol. % pyro, which was previously found to be the optimum for Dox release [33]. NIR-induced IRT release was compared to Dox release in 50% serum, and was found to be substantially faster (**Fig 1B**). To help understand these differences between IRT and Dox, cryo-transmission electron microscopographs of IRT and Dox loaded PoP liposomes comprising DSPC:DSPE-PEG2000:Pyro-lipid:Cholesterol (molar ratio 58:5:2:35) were examined. The images showed that IRT loaded liposomes did not form large elongated crystals like Dox, nor did they have an effect on the shape of the liposomes. Instead, IRT formed precipitates that occupied the entirety of the liposomes core (**Fig 2**).

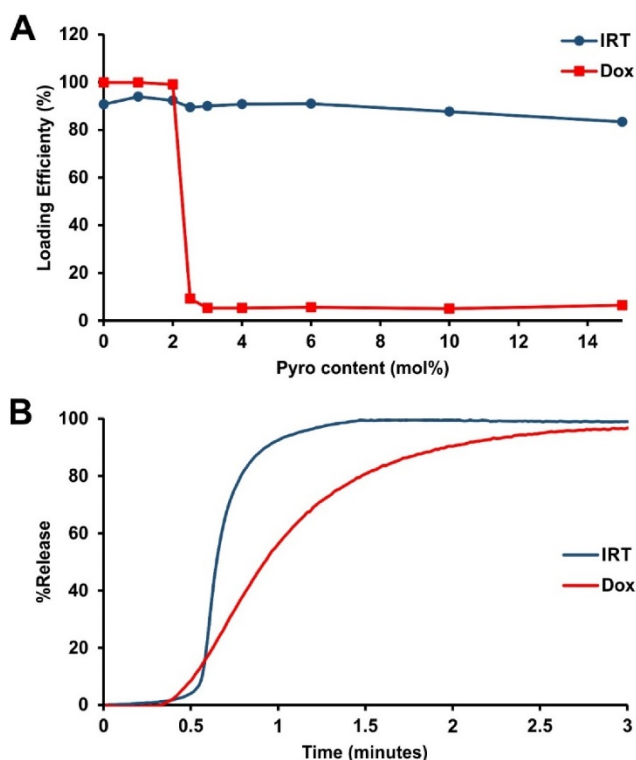


Figure 1: Drug loading and light-triggered release. A) Pyro lipid was titrated into liposomes consisting of DSPC:DSPE-PEG2000:Chol (molar ratio 60:5:35), replacing DSPC. Using this formulation Dox cannot be loaded above 2 mol. % while IRT does not demonstrate such a limitation. Data represent the average of 3 experiments (Dox data in figure A was adapted from ref. [33]) **B)** Light-induced release of Dox and IRT under 665 nm irradiation from liposomes containing 2% pyro-lipid.

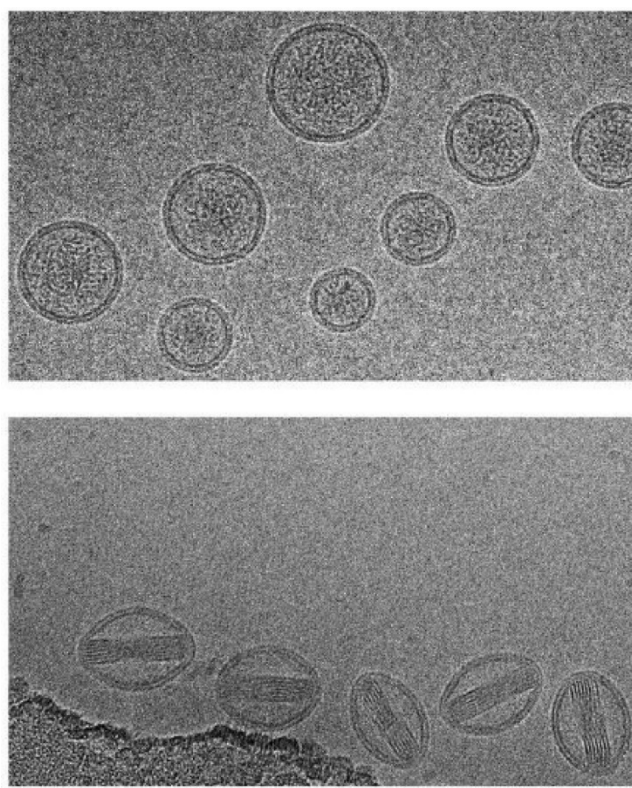


Figure 2: Effects of drug loading on liposome morphology. Cryo-TEM images of IRT (top) and Dox (bottom) loaded via an internal ammonium sulfate gradient in PoP-liposomes consisting of [DSPC:DSPE-PEG2000:Pyro-lipid:Chol] [58:5:2:35]. IRT liposomes show aggregates in the core while Dox shows linear crystals which cause the liposomes to stretch. A 50 nm scale bar is shown.

This demonstrates that IRT did not alter the shape of the liposomes. It also suggests that the poor loading of Dox in pyro-lipid containing liposomes is likely caused by destabilization of the bilayer as a consequence of the stretching induced by the formation of Dox crystals. It additionally suggests that the faster release of IRT may be due to more diffused drug aggregates inside the liposome which can dissolve more readily when the liposome bilayer is permeabilized by NIR light.

3.2 Formulation Optimization

While the formulation used in the imaging and initial experiments was stable in 50% serum when loaded with Dox, it was not stable when loaded with IRT. To address this, the cholesterol content was increased to 45 mol. % to produce more stable liposome bilayers. However, this did not significantly improve the stability. IRT is known to be prone to poor stability in liposomes [44]. One method which has been shown to enhance the stability of drug loaded liposomes is the use sphingomyelin (SPM) in place of DSPC [52,53]. To assess the effect of SPM on stability, liposomes made with SPM and DSPC were compared. DSPC liposomes were prepared using DSPC:DSPE-PEG2000:Pyro-lipid:Chol (48:5:2:45), and

SPM liposomes with SPM:DSPE-PEG2000:Pyro-lipid:Chol (48:5:2:45). The DSPC liposomes had >90% loading, whereas the SPM liposomes loaded only ~75% IRT. To verify how the absence of PEG would impact loading, we tested the loading of a PEG free SPM formulation; SPM:Pyro-lipid:Chol (53:2:45). Similar to the DSPC formulation, this formulation showed >90% loading (Fig 3A). The stability of the three formulations was compared by incubating the samples in 50% serum at 37°C. The DSPC formulation showed more than 50% release after 3 hours while both formulations with SPM had less than 30% (Fig 3B). Light triggered release experiments of IRT from these liposomes showed that the PEG-free SPM formulation had the fastest release rate, releasing most of the drug in less than 60 seconds. The PEGylated SPM formulation took 3 minutes to achieve the same results, while the DSPC formulation was significantly slower (Fig 3C). The observed lag time at the initiation of light-triggered release is likely related to initial disruption of the actively loaded IRT-sulfate aggregates inside the liposomes. Since the PEG-free SPM formulation showed good loading, greater serum stability, and faster release compared to the DSPC containing liposomes it was selected to be used for *in vivo* tests. All of the liposomes had similar

sizes and zeta potential with the exception of the SPM:Pyro-lipid:Chol liposomes which had a less negative zeta potential (**Supporting Fig S1**). To better understand the release properties, IRT release was tested under various conditions including different serum content, fluence rates and irradiation conditions. The light-triggered release rate was found to increase with increasing serum concentration, suggesting the presence of serum proteins help to destabilize the bilayer during release (**Supporting Fig S2A**). Laser treatment was essential for rapid drug release, with release starting when the laser was applied and stopping when the laser was stopped (**Supporting Fig S2B**), a phenomena which has previously been described for PoP liposomes. [31] IRT release was also found to be a function of total applied fluence rate, requiring approximately 20 J/cm² to achieve 90% release. (**Supporting Fig S2C**)

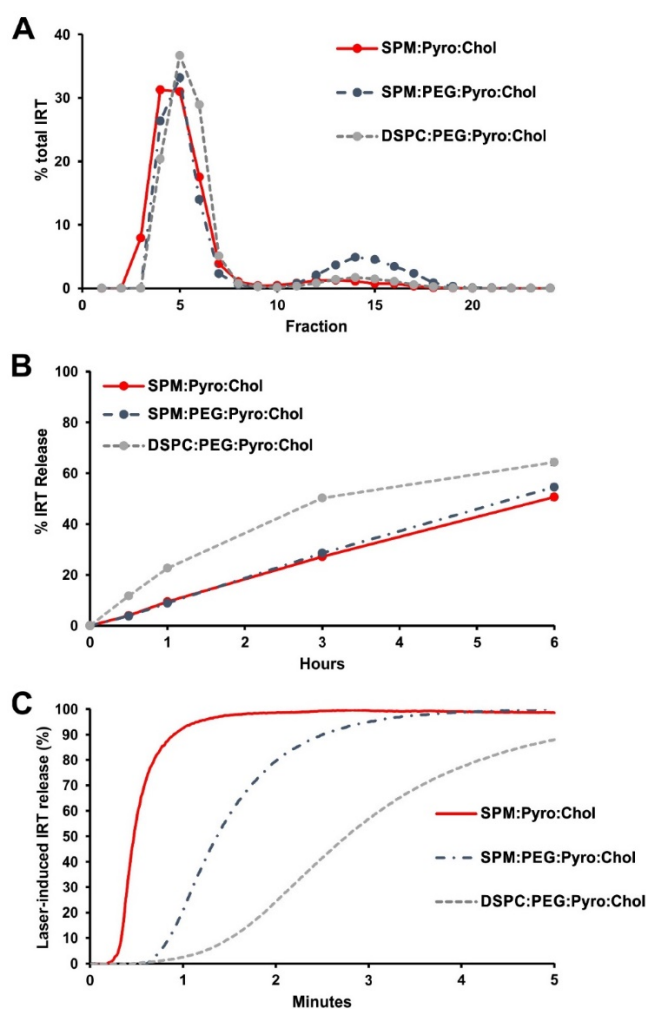


Figure 3: Development of a PoP IRT formulation. Liposomes were made with SPM:pyro-lipid:chol (53:2:45), SPM:DSPE-PEG2000:pyro-lipid:chol (48:5:2:45), or DSPC:DSPE-PEG2000:pyro-lipid:chol (48:5:2:45). **A**) IRT loading was quantified via gel filtration with a Sephadex G-75 column **B**) Stability tests in 50% adult bovine serum at 37°C. **C**) NIR-induced IRT release in 50% adult bovine serum showed SPM liposomes had faster release rate, with the PEG free formulation releasing the quickest.

3.3 Intravascular, light-triggered IRT release

We have previously shown that the efficacy of PoP liposomes is due to a combination of an vascular photodamage-related enhanced drug uptake and light-triggered release [32]. However, the extent of light-triggered drug release occurring in the vasculature was not determined, as the release rate of Dox was relatively slow. To determine whether or not vascular release was possible with this formulation, we studied the effects of laser treatment on drug release in the ears of mice as this allows for easy treatment and microscope imaging. Nude mice were injected with 10 mg/kg IRT loaded liposomes and treated on one ear. To demonstrate release was a result of laser treatment, IRT fluorescence was monitored in real time. Immediately following injection mice were anaesthetized and placed on the microscope stage and one ear treated with a laser. Mice treated with IRT PoP showed an increase in IRT fluorescence than those treated with Empty PoP + IRT liposomes ([SPM:Pyro-lipid:Chol] [53:2:45]) when the laser was turned on. (**Fig 4A**; Additional File 2: **video 1** and Additional File 3: **video 2**). Interestingly, this fluorescence decreased over time while the pyro PoP fluorescence remained relatively constant (**Fig 4B**). This suggests that the IRT was released from the liposomes and was either diffusing throughout the treated region or being washed out. While there was a difference in the IRT fluorescence between the treated and untreated ears no such difference was observed for pyro (**Supporting Fig S3**). Drug release began immediately following the start of laser treatment. This is demonstrated by a significant increase in IRT fluorescence. Over time, the fluorescence levels reached a maximum after which fluorescence began to decrease. After the end of laser treatment, the fluorescence decreased to the levels similar to the initial. However further studies are required to determine if this decrease was due to the IRT washing out or due to photobleaching from prolonged light exposure. It is most likely to be washout as the physiology of the ear vasculature and tissues may not allow for retention of the drug.

To further demonstrate that the increase in fluorescence observed was due to drug release and not liposome accumulation, pyro-lipid free liposomes ([DSPC:DSPE-PEG2000:Chol] [55:5:45]) loaded with IRT was co-injected with empty PoP-liposomes ([SPM:Pyro-lipid:Chol] [53:2:45]). The results showed no significant increase in the IRT fluorescence compared to the no laser control (**Figure S4** in the Supporting Information).

3.4 Chemophototherapy efficacy

To study the efficacy of the liposomes nude mice bearing Mia PaCa-2 tumors were injected with 15 mg/mL of free or PoP-liposome encapsulated IRT or equivalent (PoP) doses of empty liposomes and treated 10-15 minutes' post injection with a 665 nm laser at a fluence rate of 300 mW/cm² for 16 minutes, 40 seconds (300 J/cm²). As shown in Fig 5, mice treated with free IRT (median survival 18 days) showed no significant improvement over the saline control (median survival 17 days), while mice receiving IRT loaded PoP-liposomes with and without laser treatment and empty PoP-liposomes with laser showed statistically significant improvement over the saline control ($P < 0.01$). Mice receiving laser treatment and IRT-loaded PoP-liposomes showed complete tumor regression in all but one mouse (80% cure rate). Mice receiving only IRT-loaded PoP-liposomes without laser treatment and empty PoP-liposome with laser treatment had median survival times of 29 days and 42 (with 17 % cured) days respectively. There was no statistically significant difference between these two groups; however, there was a significant difference between each group and the IRT loaded PoP-liposomes and laser treatment ($P < 0.05$).

Individual tumor growth curves are shown in Figure S5 in the Supporting Information. This demonstrates a synergistic effect between the laser treatment and drug delivery which together produce an overall effective chemophototherapy treatment. Photodynamic therapy is known to be able to enhance the permeability of nanoparticles in tumor vasculature and affect blood flow [54–56]. We have previously shown that both effects are present in tumors treated with Dox PoP-liposomes [33] and would expect similar effects to be present in IRT PoP liposomes. The results of the survival study for IRT PoP liposomes are similar to that of Dox PoP liposomes with the empty +laser and Dox PoP -laser having equal efficacy and the Dox/IRT PoP liposomes showing significantly greater efficacy. The improved efficacy of the IRT-PoP +laser can be attributed to a synergistic effect between the drug and the photodynamic effects similar to that previously observed for Dox PoP liposomes. Microscopy images of tumors treated with IRT PoP with and without laser show that tumors receiving laser treatment had a greater and more homogeneous distribution of IRT (Supporting Fig S6).

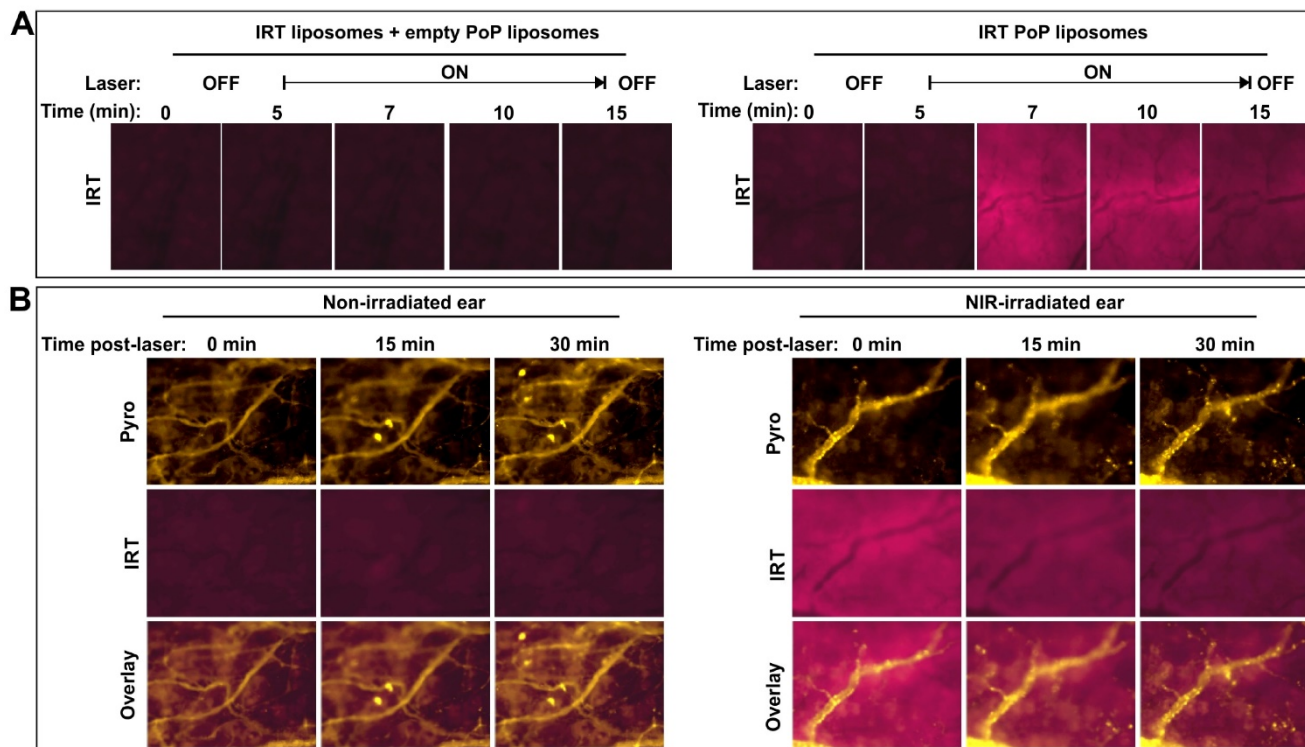


Figure 4: Intravascular light-triggered IRT release. Mice were injected with SPM:pyro-lipid:chol liposomes loaded with IRT (10 mg/kg IRT), anaesthetized and treated on one ear with a 665 nm laser at a fluence rate of 300 mW/cm². **A)** IRT fluorescence was measured during treatment in mice injected with both empty PoP-liposomes and PoP-free IRT loaded liposomes (left) or IRT loaded PoP liposomes (right). **B)** Pyro-lipid and IRT fluorescence were also monitored immediately following a 10 minute phototreatment.

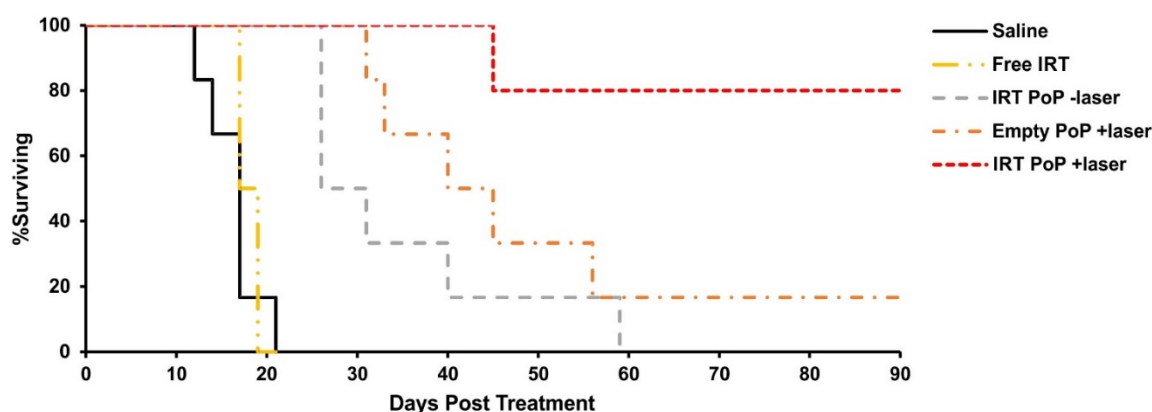


Figure 5: Kaplan-Meier survival curves for nude mice bearing Mia PaCa-2 tumors phototreated shortly after IV injection. Mice were IV injected with saline, 15 mg/kg free IRT, 15 mg/kg IRT-loaded PoP liposomes or equivalent PoP doses of empty liposomes. 10 minutes following injection, mice in the +laser groups were treated with a 665 nm laser at a fluence rate of 300 mW/cm² for 16 min. 40 sec. (300 J/cm²). Mice were given a single treatment and sacrificed when the tumors grew more than 10 times initial size. n= 5-7 mice per group.

Conclusion

We demonstrated that IRT can be loaded into liposomes with higher pyro-lipid content, whereas that was not possible for Dox. This is likely linked to the morphology of the liposomes following loading, and the avoidance of bilayer stretching by IRT. While IRT was loaded effectively into PoP liposomes, IRT loaded liposomes were not as stable as Dox loaded liposomes. IRT has been reported to be unstable in liposomes and strategies are being developed to increase stability and efficacy [44,49,50,57-59]. In this work, we substituted the DSPC used in our previous formulation with sphingomyelin, increased the cholesterol content and omitted PEG. This approach resulted in liposomes with a modest increase in serum stability. Although the liposomes were not highly serum stable, when subjected to NIR light treatment, they rapidly released the drug and effectively suppressed tumor growth. Taken together, we conclude that IRT PoP liposomes are promising for chemophototherapy approaches.

Supplementary Material

Additional File 1:

Figures S1-S6. <http://www.thno.org/v06p2329s1.pdf>

Additional File 2:

Video 1. <http://www.thno.org/v06p2329s2.wmv>

Additional File 3:

Video 2. <http://www.thno.org/v06p2329s3.wmv>

Acknowledgments

This work was supported by the National Institutes of Health (R01EB017270 and DP5OD017898).

Competing Interests

The authors have declared that no competing

interest exists.

References

- Torchilin VP. Recent advances with liposomes as pharmaceutical carriers. *Nat. Rev. Drug Discov.* 2005;4:145-60.
- Peer D, Karp JM, Hong S, Farokhzad OC, Margalit R, Langer R. Nanocarriers as an emerging platform for cancer therapy. *Nat. Nanotechnol.* 2007;2:751-60.
- Wang AZ, Langer R, Farokhzad OC. Nanoparticle Delivery of Cancer Drugs. *Annu. Rev. Med.* 2012;63:185-98.
- Allen TM, Cullis PR. Drug Delivery Systems: Entering the Mainstream. *Science.* 2004;303:1818-22.
- Maruyama K. Intracellular targeting delivery of liposomal drugs to solid tumors based on EPR effects. *Adv. Drug Deliv. Rev.* 2011;63:161-9.
- Fang J, Nakamura H, Maeda H. The EPR effect: Unique features of tumor blood vessels for drug delivery, factors involved, and limitations and augmentation of the effect. *Adv. Drug Deliv. Rev.* 2011;63:136-51.
- Torchilin V. Tumor delivery of macromolecular drugs based on the EPR effect. *Adv. Drug Deliv. Rev.* 2011;63:131-5.
- Maeda H. Macromolecular therapeutics in cancer treatment: The EPR effect and beyond. *J. Controlled Release.* 2012;164:138-44.
- Barenholz Y. Doxil® – The first FDA-approved nano-drug: Lessons learned. *J. Controlled Release.* 2012;160:117-34.
- Manzoor AA, Lindner LH, Landon CD, Park J-Y, Simnick AJ, Dreher MR, et al. Overcoming Limitations in Nanoparticle Drug Delivery: Triggered, Intravascular Release to Improve Drug Penetration into Tumors. *Cancer Res.* 2012;72:5566-75.
- Prabhakar U, Maeda H, Jain RK, Sevick-Muraca EM, Zamboni W, Farokhzad OC, et al. Challenges and Key Considerations of the Enhanced Permeability and Retention Effect for Nanomedicine Drug Delivery in Oncology. *Cancer Res.* 2013;73:2412-7.
- Jain RK, Stylianopoulos T. Delivering nanomedicine to solid tumors. *Nat. Rev. Clin. Oncol.* 2010;7:653-64.
- Bertrand N, Wu J, Xu X, Kamaly N, Farokhzad OC. Cancer nanotechnology: The impact of passive and active targeting in the era of modern cancer biology. *Adv. Drug Deliv. Rev.* 2014;66:2-25.
- Mills JK, Needham D. Targeted drug delivery. *Expert Opin. Ther. Pat.* 1999;9:1499-513.
- Koo OM, Rubinstein I, Onyuksel H. Role of nanotechnology in targeted drug delivery and imaging: a concise review. *Nanomedicine Nanotechnol. Biol. Med.* 2005;1:193-212.
- Freeman AI, Mayhew E. Targeted drug delivery. *Cancer.* 1986;58:573-83.
- Ganta S, Devalapally H, Shahiwala A, Amiji M. A review of stimuli-responsive nanocarriers for drug and gene delivery. *J. Controlled Release.* 2008;126:187-204.
- Luo D, Carter KA, Lovell JF. Nanomedical engineering: shaping future nanomedicines. *Wiley Interdiscip. Rev. Nanomed. Nanobiotechnol.* 2015;7:169-88.
- You J, Zhang G, Li C. Exceptionally High Payload of Doxorubicin in Hollow Gold Nanospheres for Near-Infrared Light-Triggered Drug Release. *ACS Nano.* 2010;4:1033-41.
- Timko BP, Kohane DS. Prospects for near-infrared technology in remotely triggered drug delivery. *Expert Opin. Drug Deliv.* 2014;11:1681-5.
- Araki T, Ogawara K, Suzuki H, Kawai R, Watanabe T, Ono T, et al. Augmented EPR effect by photo-triggered tumor vascular treatment improved therapeutic efficacy of liposomal paclitaxel in mice bearing tumors with low permeable vasculature. *J. Controlled Release.* 2015;200:106-14.

22. Fomina N, Sankaranarayanan J, Almutairi A. Photochemical mechanisms of light-triggered release from nanocarriers. *Adv. Drug Deliv. Rev.* 2012;64:1005–20.
23. Zhen Z, Tang W, Chen H, Lin X, Todd T, Wang G, et al. RGD-Modified Apoferritin Nanoparticles for Efficient Drug Delivery to Tumors. *ACS Nano.* 2013;7:4830–7.
24. He C, Liu D, Lin W. Self-Assembled Core-Shell Nanoparticles for Combined Chemotherapy and Photodynamic Therapy of Resistant Head and Neck Cancers. *ACS Nano.* 2015;9:991–1003.
25. Spring BQ, Sears RB, Zheng LZ, Mai Z, Watanabe R, Sherwood ME, et al. A photoactivable multi-inhibitor nanoliposome for tumour control and simultaneous inhibition of treatment escape pathways. *Nat. Nanotechnol.* 2016;11:378–87.
26. Yen H-C, Cabral H, Mi P, Toh K, Matsumoto Y, Liu X, et al. Light-Induced Cytosolic Activation of Reduction-Sensitive Camptothecin-Loaded Polymeric Micelles for Spatiotemporally Controlled in Vivo Chemotherapy. *ACS Nano.* 2014;8:11591–602.
27. Luo D, Carter KA, Miranda D, Lovell JF. Chemophototherapy: An Emerging Treatment Option for Solid Tumors. *Adv. Sci.* 2016.
28. Huang H, Song W, Rieffel J, Lovell JF. Emerging applications of porphyrins in photomedicine. *Front. Phys.* 2015;3:23.
29. Zhang Y, Lovell JF. Porphyrins as theranostic agents from prehistoric to modern times. *Theranostics.* 2012;2:905–15.
30. Zhang Y, Lovell JF. Recent applications of phthalocyanines and naphthalocyanines for imaging and therapy. *Wiley Interdiscip. Rev. Nanomed. Nanobiotechnol.* 2016.
31. Carter KA, Shao S, Hoopes MI, Luo D, Ahsan B, Grigoryants VM, et al. Porphyrin-phospholipid liposomes permeabilized by near-infrared light. *Nat. Commun.* 2014; 5:3546.
32. Luo D, Carter KA, Razi A, Geng J, Shao S, Lin C, et al. Porphyrin-phospholipid liposomes with tunable leakiness. *J. Controlled Release.* 2015;220:484–94.
33. Luo D, Carter KA, Razi A, Geng J, Shao S, Giraldo D, et al. Doxorubicin encapsulated in stealth liposomes conferred with light-triggered drug release. *Biomaterials.* 2016;75:193–202.
34. Lovell JF, Jin CS, Huynh E, Jin H, Kim C, Rubinstein JL, et al. Porphysome nanovesicles generated by porphyrin bilayers for use as multimodal biophotonic contrast agents. *Nat. Mater.* 2011;10:324–32.
35. Carter KA, Wang S, Geng J, Luo D, Shao S, Lovell JF. Metal Chelation Modulates Phototherapeutic Properties of Mitoxantrone-Loaded Porphyrin-Phospholipid Liposomes. *Mol. Pharm.* 2016;13:420–7.
36. Shao S, Geng J, Ah Yi H, Gogia S, Neelamegham S, Jacobs A, et al. Functionalization of cobalt porphyrin-phospholipid bilayers with his-tagged ligands and antigens. *Nat. Chem.* 2015;7:438–46.
37. Kress J, Rohrbach DJ, Carter KA, Luo D, Shao S, Lele S, et al. Quantitative imaging of light-triggered doxorubicin release. *Biomed. Opt. Express.* 2015;6:3546–55.
38. Rieffel J, Chen F, Kim J, Chen G, Shao W, Shao S, et al. Hexamodal Imaging with Porphyrin-Phospholipid-Coated Upconversion Nanoparticles. *Adv. Mater.* 2015;27:1785–90.
39. Luo D, Li N, Carter KA, Lin C, Geng J, Shao S, et al. Rapid Light-Triggered Drug Release in Liposomes Containing Small Amounts of Unsaturated and Porphyrin-Phospholipids. *Small.* 2016;12:3039–47.
40. Lovell JF, Jin CS, Huynh E, MacDonald TD, Cao W, Zheng G. Enzymatic Regioselection for the Synthesis and Biodegradation of Porphysome Nanovesicles. *Angew. Chem. Int. Ed.* 2012;51:2429–33.
41. Fritze A, Hens F, Kimpfler A, Schubert R, Peschka-Süss R. Remote loading of doxorubicin into liposomes driven by a transmembrane phosphate gradient. *Biochim. Biophys. Acta BBA - Biomembr.* 2006;1758:1633–40.
42. Lasic DD, Frederik PM, Stuart MCA, Barenholz Y, McIntosh TJ. Gelation of liposome interior: A novel method for drug encapsulation. *FEBS Lett.* 1992;312:255–8.
43. Andriyanov AV, Koren E, Barenholz Y, Goldberg SN. Therapeutic Efficacy of Combining PEGylated Liposomal Doxorubicin and Radiofrequency (RF) Ablation: Comparison between Slow-Drug-Releasing, Non-Thermosensitive and Fast-Drug-Releasing, Thermosensitive Nano-Liposomes. *PLoS ONE.* 2014;9:e92555.
44. Chou T-H, Chen S-C, Chu I-M. Effect of Composition on the stability of liposomal irinotecan prepared by a pH gradient method. *J. Biosci. Bioeng.* 2003;95:405–8.
45. Messerer CL, Ramsay EC, Waterhouse D, Ng R, Simms E-M, Harasym N, et al. Liposomal Irinotecan Formulation Development and Therapeutic Assessment in Murine Xenograft Models of Colorectal Cancer. *Clin. Cancer Res.* 2004;10:6638–49.
46. Drummond DC, Noble CO, Guo Z, Hong K, Park JW, Kirpotin DB. Development of a Highly Active Nanoliposomal Irinotecan Using a Novel Intraliposomal Stabilization Strategy. *Cancer Res.* 2006;66:3271–7.
47. Mathijssen RHJ, Alphen RJ van, Verweij J, Loos WJ, Nooter K, Stoter G, et al. Clinical Pharmacokinetics and Metabolism of Irinotecan (CPT-11). *Clin. Cancer Res.* 2001;7:2182–94.
48. Chang H-I, Yeh M-K. Clinical development of liposome-based drugs: formulation, characterization, and therapeutic efficacy. *Int. J. Nanomedicine.* 2012;7:49–60.
49. Ramsay E, Alnajim J, Anantha M, Taggar A, Thomas A, Edwards K, et al. Transition Metal-Mediated Liposomal Encapsulation of Irinotecan (CPT-11) Stabilizes the Drug in the Therapeutically Active Lactone Conformation. *Pharm. Res.* 2006;23:2799–808.
50. Wei H, Song J, Li H, Li Y, Zhu S, Zhou X, et al. Active loading liposomal irinotecan hydrochloride: Preparation, in vitro and in vivo evaluation. *Asian J. Pharm. Sci.* 2013;8:303–11.
51. Li X, Mooney P, Zheng S, Booth CR, Braunfeld MB, Gubbens S, et al. Electron counting and beam-induced motion correction enable near-atomic-resolution single-particle cryo-EM. *Nat. Methods.* 2013;10:584–90.
52. Webb MS, Harasym TO, Masin D, Bally MB, Mayer LD. Sphingomyelin-cholesterol liposomes significantly enhance the pharmacokinetic and therapeutic properties of vincristine in murine and human tumour models. *Br. J. Cancer.* 1995;72:896–904.
53. Tardi P, Choice E, Masin D, Redelmeier T, Bally M, Madden TD. Liposomal encapsulation of topotecan enhances anticancer efficacy in murine and human xenograft models. *Cancer Res.* 2000;60:3389–93.
54. Snyder JW, Greco WR, Bellnier DA, Vaughan L, Henderson BW. Photodynamic therapy: a means to enhanced drug delivery to tumors. *Cancer Res.* 2003;63:8126–31.
55. Sano K, Nakajima T, Choyke PL, Kobayashi H. Markedly Enhanced Permeability and Retention Effects Induced by Photo-immunotherapy of Tumors. *ACS Nano.* 2013;7:717–24.
56. Zhen Z, Tang W, Chuang Y-J, Todd T, Zhang W, Lin X, et al. Tumor Vasculature Targeted Photodynamic Therapy for Enhanced Delivery of Nanoparticles. *ACS Nano.* 2014;8:6004–13.
57. Modrak DE, Rodriguez MD, Goldenberg DM, Lew W, Blumenthal RD. Sphingomyelin enhances chemotherapy efficacy and increases apoptosis in human colonic tumor xenografts. *Int. J. Oncol.* 2002;20:379–84.
58. Krauze MT, Noble CO, Kawaguchi T, Drummond D, Kirpotin DB, Yamashita Y, et al. Convection-enhanced delivery of nanoliposomal CPT-11 (irinotecan) and PEGylated liposomal doxorubicin (Doxil) in rodent intracranial brain tumor xenografts. *Neuro-Oncol.* 2007;9:393–403.
59. Hattori Y, Shi L, Ding W, Koga K, Kawano K, Hakoshima M, et al. Novel irinotecan-loaded liposome using phytic acid with high therapeutic efficacy for colon tumors. *J. Controlled Release.* 2009;136:30–7.